ChemMedChem

Chemistry Europe
European Chemical Societies Publishing

Accepted Article

Title: 4-Fluorobenzylpiperazine-containing derivatives as efficient inhibitors of mushroom tyrosinase

Authors: Serena Vittorio, Laura Ielo, Salvatore Mirabile, Rosaria Gitto, Antonella Fais, Sonia Floris, Antonio Rapisarda, Maria Paola Germanò, and Laura De Luca

To be cited as: *ChemMedChem* 10.1002/cmdc.202000125

Link to VoR: https://doi.org/10.1002/cmdc.202000125

WILEY-VCH

10.1002/cmdc.202000125

WILEY-VCH

FULL PAPER

4-Fluorobenzylpiperazine-containing derivatives as efficient inhibitors of mushroom tyrosinase

Serena Vittorio,[a],* Laura Ielo,[b] Salvatore Mirabile,[a] Rosaria Gitto,[a] Antonella Fais,[c] Sonia Floris,[c] Antonio Rapisarda,[a] Maria Paola Germanò [a] and Laura De Luca[a],*

[a] S. Vittorio, S. Mirabile, Prof. R. Gitto, Prof. A. Rapisarda, Prof. M. P. Germanò, Prof. L. De Luca
Department of Chemical, Biological, Pharmaceutical and Environmental Sciences
University of Messina
Viale Palatucci, 13, I-98168, Messina, Italy
E-mail: svittorio@unime.it, ldeluca@unime.it
[b] Dr. L. Ielo
Department of Pharmaceutical Chemistry
University of Vienna
Althanstrasse 14, A-1090 Vienna, Austria
[c] Dr. A. Fais, S. Floris
Department of Life and Environmental Sciences
University of Cagliari
..... I-09042 Monserrato, Cagliari, Italy

Supporting information for this article is given via a link at the end of the document.

Abstract: Tyrosinase is a type 3 copper protein involved in the biosynthesis of melanin pigments, therefore the inhibition of its enzymatic activity represents a promising strategy for the treatment of hyperpigmentation-related disorders. To address this point at issue we have previously designed a class of 4-(4-fluorobenzyl)piperazin-1-yl-based compounds proving to be more active inhibitor against tyrosinase from mushroom *Agaricus bisporus* when compared to positive control kojic acid. Herein, we report the synthesis of further series of 4-(4-fluorobenzyl)piperazin-1-yl-analogs bearing a (hetero)aromatic fragment as key feature to improve protein affinity. The new synthesized compounds were *in vitro* assayed proving to be potent inhibitors in low micromolar range. Then, the active 2-thienyl and 2-furyl derivatives were selected for further modifications considering their binding mode analyzed by docking studies and their satisfactory safety profiles.

Introduction

Melanogenesis is a multistep process resulting in the formation of melanin pigments which are responsible for skin, hair and eyes color. [1, 2] Under physiological conditions, melanin plays an important role in the protection of the skin against damaging effects of UV radiation while its over-production can cause hyper-pigmentary disorders such as melasma, freckles, post-inflammatory melanoderma, pigmented acne scars and age spots [3]. Furthermore, the biosynthetic pathway that lead to the production of neuromelanin seems to be linked to Parkinson's disease. [4,5]

Different strategies can be exploited to modulate melanogenesis including the reduction of the expression of melanogenic enzymes, the alteration of the related signalling pathways and the inhibition of tyrosinase activity. [1] Tyrosinase (EC 1.14.18.1) is a copper containing enzyme that catalyzes the rate limiting-step of melanin biosynthesis: the conversion of tyrosine in L-DOPA and its oxidation in o-dopaquinone.[6, 7] Its active site contains a binuclear copper center with six histidine residues involved in the coordination of the two metal ions[8]. The inhibition of tyrosinase activity is a widely used strategy for blocking melanogenesis thus reducing melanin synthesis.[9, 10] Tyrosinase inhibitors such as kojic acid and arbutin are employed by pharmaceutical and cosmetic industries as active ingredients for the preparation of skin-whitening formulations, but they have shown low efficacy, low stability and cytotoxicity.[11, 12, 13] Particularly, it has been clearly demonstrated that kojic acid is poor human tyrosinase inhibitor. Moreover, it has been reported that several tyrosinase inhibitors, both from synthetic [14] and natural sources, possess antibacterial activity. [9] In bacteria, melanin exerts a protective role against UV radiation, chelates metals in stress conditions and neutralize the effects of antibiotics, thus increasing cell viability. Therefore, the inhibition of tyrosinase activity and the subsequent reduction of melanin synthesis could be exploited as strategy for the development of new antibiotics. However, more efforts are needed in order to clarify the mechanism that correlates the antimicrobial effect with the inhibition of melanin synthesis.[9] For these reasons there is a growing interest in the search of more effective and potent tyrosinase inhibitors.[11, 12]

In our previous studies we have identified a new class of tyrosinase inhibitors bearing the 4-fluorobenzyl substituent as a key structural motif, which establishes favorable contacts within catalytic site in proximity of the two copper ions.[12, 15, 16] Experimental and theoretical structural investigations carried out on tyrosinases from *Bacillus megaterium* and *Agaricus bisporus* allowed us to identify 4-(4-fluorobenzyl)piperazin-1-yl](2-methylphenyl)methanone **(1a)** as promising TyI (IC_{50}=5μM) showing higher potency than the reference compound kojic acid (IC_{50}=18μM) (Figure 1).[12]

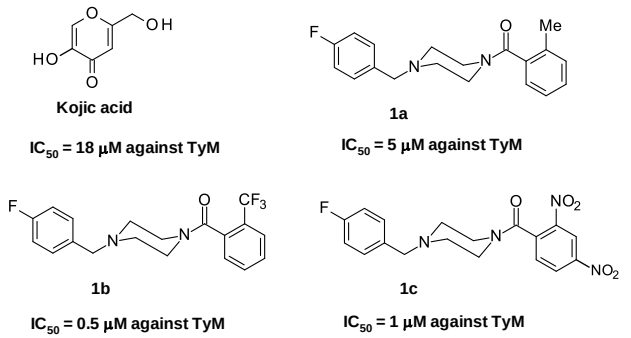

Figure 1. Tyrosinase inhibitors

As shown in Figure 2A, the docking studies[17] on mushroom tyrosinase revealed that **1a** was accommodated in the catalytic cavity through π/π stacking interactions with His263 as well as hydrophobic contacts with Val283, Met257, Val284 and Phe264. In turn, the binding pose was used as starting point for the generation of Apo-site pharmacophore grids (Figure 2B), which suggested suitable hydrophobic and hydrophilic substituents. In particular, we designed a further series of 4-fluorobenzylpiperazine compounds, in which the benzoyl moiety was properly decorated. As result, we obtained improved inhibitory activity toward *Agaricus bisporus* tyrosinase up to submicromolar range as showed by compounds **1b** and **1c** (0.5 and 1 µM, see Figure 1),[17] thus confirming our computational hypotheses.

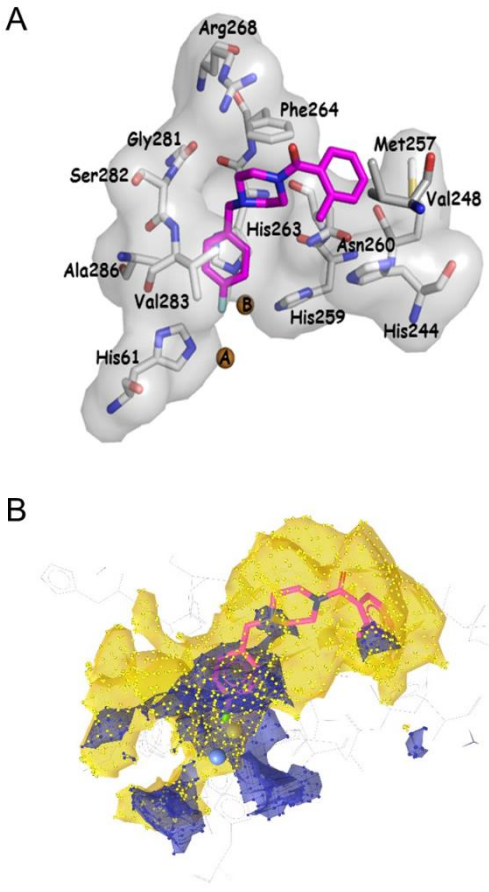

Figure 2. (A) Apo Site Grid generated starting from the best docking pose of derivative **1a** in the catalytic site of *Agaricus bisporus* tyrosinase. (B) Yellow grid highlights the favorable presence of hydrophobic groups and specifically blue grid indicates aromatic rings. The picture was generated using Ligand Scout software.[18]

In coherence with these previous findings, in this study we replaced the 2-tolyl substituent of prototype **1a** with further chemical moieties able to establish favorable hydrophobic contacts. All the designed compounds were synthesized and tested for their ability to inhibit tyrosinase activity, and the cytotoxicity was determined for selected compounds. Moreover, docking simulations were performed to clarify the binding mode into the mushroom tyrosinase active site.

Results and Discussion

We chose to probe the effect of the substitution of benzoyl moiety linked to the piperazine ring with other (hetero)aromatic systems as shown for the seven 4-(4-fluorobenzyl)piperazin-1-yl-based derivatives **2a-g** depicted in Figure 3.

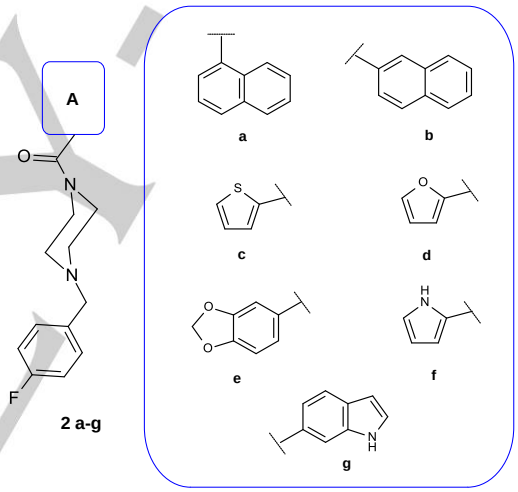

Figure 3. Designed compounds **2a-g** structurally related to prototype **1**.

For each designed molecule we preliminarily estimated several selected chemical-physical parameters related to the pharmacokinetic behavior of a drug in the biological systems, like topological polar surface area (TPSA), pKa, logP and logD at pH =7 by using the web tool Chemicalize (www.chemicalize.it) with the aim to synthesize compounds with drug-like properties (see Supporting Information Table S1). Furthermore, we found that all the compounds respected the rules of Lipinski and no PAINS were predicted by the online free tool SwissAdme (http://www.swissadme.ch/).

So, the designed compounds **2a-g** were synthesized starting from 4-(4-fluorobenzyl)piperazine **3** that was coupled with the suitable acyl chloride (RCOCl) or carboxylic acid derivative (RCOOH) to obtain **2a-e** and **2f-g**, respectively (Scheme 1). The mixture reaction was initially stirred at room temperature for 5 hours or left overnight.

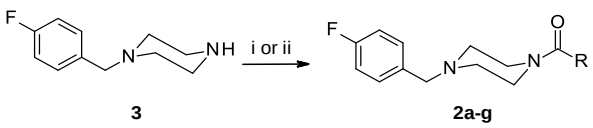

3 2a-g

	R
a	1-naphthyl
b	2-naphthyl
c	2-thienyl
d	2-furyl
e	1,3-dioxol-5-yl
f	2-pyrrolyl
g	6-indolyl

Scheme 1. Reagents and conditions: i) RCOCl, DIPEA, DCM, MW: 10 min, 50 °C, 200 W; ii) RCOOH, HBTU, TEA, DMF, MW: 10 min, 50 °C, 200 W.

In order to optimize the synthetic procedure, the reactions were carried out for 10 minutes at 50 °C in the microwave conditions, with an evident reduction of the times and improvement of the yields. ^{1}H and ^{13}C NMR spectra data of compounds were in full agreement with the proposed structures and representative data are shown in Supporting Information.

Agaricus bisporus tyrosinase was used to evaluate *in vitro* inhibitory effects of compounds **2a-g** using L-DOPA as substrate. The activities were expressed as IC_{50} values and were summarized in Table 1. For comparison purpose, the IC_{50} values of parent compound **1a** and kojic acid (KA) are shown in Table 1.

Table 1. Inhibitory activity of compounds **2a-g** compared to inhibitor **1** and kojic acid as reference compounds.

Cpd	Diphenolase activity IC_{50} (μM)[a]
2a	3±0.4
2b	3±1.1
2c	3±0.6
2d	5±0.5
2e	3±0.1
2f	12±3.5
2g	5±0.9
1a	5±1.6
Kojic acid	18±0.2

[a] IC_{50} values represent the concentration that caused 50% enzyme activity loss. All compounds were studied in a set of experiments performed in three replicates.

The replacement of the 2-tolyl substituent of prototype **1a** by (hetero)aromatic rings generally led to more active compounds with the exception of 2-pyrrolyl substituted derivative **2f**, displaying a slight decrease of inhibitory effects. Notably, all tested compounds proved to be more potent than reference compound kojic acid.

Considering the possibility to further exploring this class of compounds, we focused our attention on active inhibitors **2c** and **2d**. Before starting with the structural modification on selected compounds, the cytotoxicity of 2-thienyl substituted compound **2c** was carried out to determine the safety of this molecule (Figure 4A). Cells were treated with different concentration of inhibitor (4–100 μM) for 48 h and were examined using MTT test. The results indicated that **2c** exhibited no cytotoxic effect in HeLa cells at the IC_{50} value. The same protocol was applied for 2-furyl substituted compound **2d** and non-cytotoxicity was revealed as shown in Figure 4B.

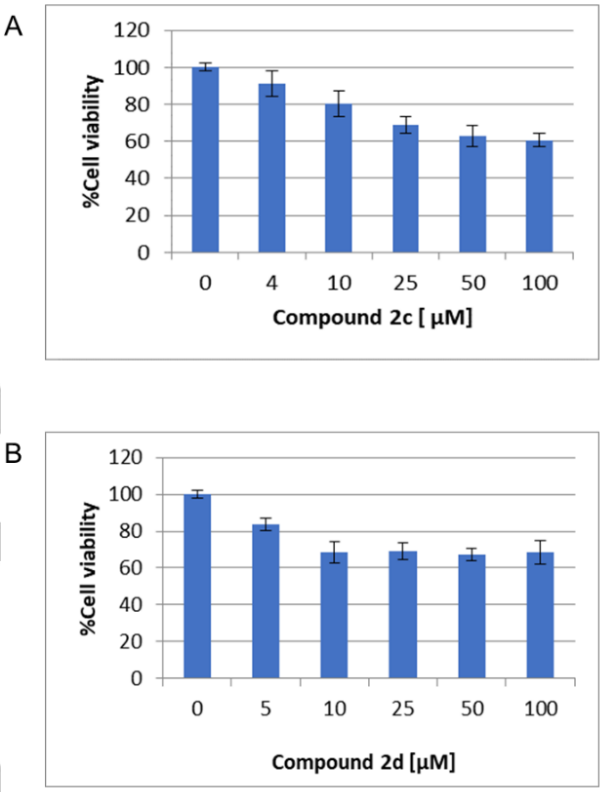

Figure 4. The effect of compounds **2c** (A) and **2d** (B) on HeLa cell viability. Cells were treated with different concentrations for compound **2c** (4-100 μM) and for compound **2d** (5-100 μM) and their viability was evaluated by MTT assay.

Furthermore, docking studies of **2c** and **2d** were performed into mushroom tyrosinase active site (PDB code 2Y9X) [19] by Gold software[20] in order to have information about their binding mode. As displayed in Figure 5, the two inhibitors shared a very similar binding mode with the p-fluorobenzyl moiety oriented towards the copper ions, establishing hydrophobic contacts with Val283 and π-stacking interaction with His263 as reported above for prototype **1a**. Instead, the 2-furyl and 2-thienyl rings are involved in hydrophobic interactions with Phe264.

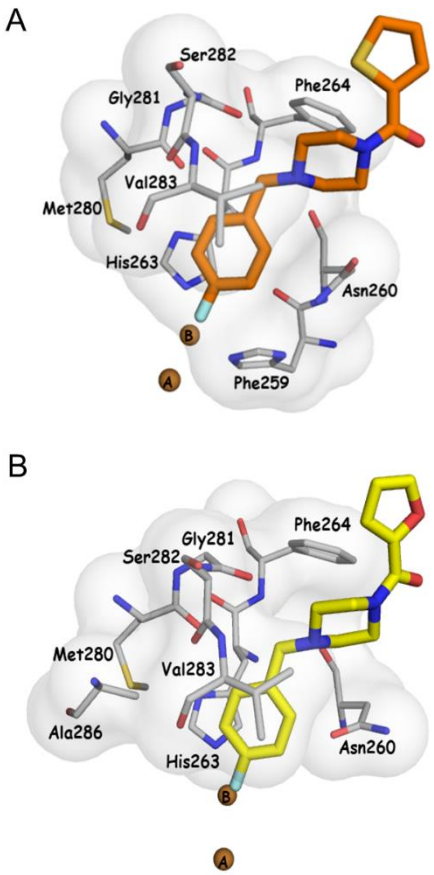

Figure 5. Plausible binding mode for inhibitors **2c** (Panel A) and **2d** (Panel B). Compounds **2c** (ΔG_{bind}=-22.38 kcal/mol) and **2d** (ΔG_{bind}=-21.27 kcal/mol) are represented respectively as orange and yellow sticks. Key residues of the binding site are depicted as white stick. Copper ions are represented as brown spheres. The images are created by means of PyMOL (https://pymol.org).

To improve the inhibitory properties of 2-thienyl and 2-furyl substituted compounds, we introduced slight structural modifications depicted in Scheme 2: (a) lengthening of carbon spacer between piperazine core and heterocyclic fragment (*e.g.* compounds **2h-i**); (b) replacement of 2-thienyl or 2-furyl ring with corresponding benzothiophene and benzofuran nucleus (*e.g.* compounds **2j-k**); (c) introduction of different substituents on thiophene ring (*e.g.* compounds **2l-p**) or furan ring (*e.g.* compounds **2q-s**). As done for **2a-g**, we estimated chemical-physical parameters for this second series of designed molecules **2h-s** (Supporting Information Table S1). These new derivatives depicted in Scheme 2 were prepared following the same synthetic procedure described in Scheme 1 for compounds **2a-g**. Specifically, to prepare compounds **2h**, **2k-m**, **2q-s** we used heteroaroyl chloride (RCOCl) as starting material; whereas for **2i**, **2j**, **2n-p** we employed the corresponding carboxylic derivative (RCOOH).

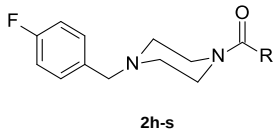

2h-s

	R
h	2-thienylmethyl
i	2-furylmethyl
j	benzothiophen-2-yl
k	benzofuran-2-yl
l	3-methylthiophen-2-yl
m	4-methylthiophen-2-yl
n	3-bromothiophen-2-yl
o	5-chlorothiophen-2-yl
p	5-nitrothiophen-2-yl
q	3-methylfuran-2-yl
r	5-methylfuran-2-yl
s	5-nitrofuran-2-yl

Scheme 2. The synthesized compounds **2h-s** were prepared as reported for analogues **2a-g.**

The inhibitory activities of this further series of compounds are summarized in Table 2. Overall, the performed structural modifications did not significantly affect the IC_{50} values respect to their parent compounds **2c-d**. In detail, the lengthening of carbon spacer (**2h-i**) as well as the introduction of specific substituents on crucial position of heterocyclic system (*e.g.* **2m**, **2o**, and **2q**) gave an unpredictable reduction of the inhibitory effects; conversely, the benzene-fused derivatives **2j-k** proved to maintain potent inhibitory effects in the low micromolar range.

Table 2. Inhibitory activity of compounds **2h-s** compared to inhibitor **1** and kojic acid as reference compounds

Cpd	Diphenolase activity IC_{50} (μM)[a]
2h	14 ± 2.8
2i	18 ± 2.1
2j	4 ±0.3
2k	5 ±0.8
2l	8± 1.4
2m	19 ± 3.5
2n	3 ±0.4
2o	32 ± 6.1
2p	3 ± 0.2
2q	42 ± 13.6
2r	3.3 ± 1.0
2s	12 ± 1.3
1a	5 ± 1.6
Kojic acid	18 ± 0.2

[a] IC_{50} values represent the concentration that caused 50% enzyme activity loss. All compounds were studied in a set of experiments performed in three replicates.

Conclusion

Herein, we reported the design and synthesis of a new series of tyrosinase inhibitors bearing the 4-(4-fluorobenzyl)piperazine fragment, by introducing (hetero)aromatic moieties in the place of the o-tolyl group of prototype **1a**. All the obtained compounds showed significant inhibitory activity against tyrosinase from *Agaricus bisporus*. Among this new series of tyrosinase inhibitors, derivatives **2c** and **2d** were selected as new lead compounds for further chemical explorations. Cell viability assays revealed that **2c** and **2d** showed no considerable cytotoxic effects in HeLa cells. Furthermore, docking studies clarified the binding mode of these two inhibitors highlighting an interaction network similar to that of prototype **1a**. With the aim to improve the inhibitory activity of **2c** and **2d**, we carried out structural modifications thus collecting

additional SAR considerations for this series of compounds. As mushroom and human tyrosinases have shown distinct active site interaction patterns leading to very different inhibition values, [21, 22] additional experiments using human tyrosinase or human melanoma or melanocyte cells are needed to support the potential of these compounds for human-directed applications.

Experimental Section

Chemistry

All reagents were used without further purification and bought from common commercial suppliers (Sigma-Aldrich, Milan, Italy and Alfa Aesar, Karlsruhe, Germany). Microwave-assisted reactions were carried out in a Focused Microwawe TM Synthesis System, Model Discover (CEM Technology Ltd Buckingham, UK). Melting points were determined on a Buchi B-545 apparatus (BUCHI Labortechnik AG Flawil, Switzerland) and are uncorrected. By combustion analysis (C, H, N) carried out on a Carlo Erba Model 1106-Elemental Analyzer we determined the purity of synthesized compounds; the results confirmed a ≥95% purity. Merck Silica Gel 60 F254 plates were used for analytical thin-layer chromatography (TLC; Merck KGaA, Darmstadt, Germany). Flash Chromatography (FC) was carried out on a Biotage SP1 EXP (Biotage AB Uppsala, Sweden). ^{1}H NMR spectra and ^{13}C NMR spectra were measured in dimethylsulfoxide-d6 (DMSO-d6) or chloroform ($CDCl_3$) with a Varian Gemini 500 spectrometer (Varian Inc. Palo Alto, California USA); chemical shifts are expressed in δ (ppm) and coupling constants (J) in hertz (Hz). Mass spectra of selected compounds (**2b**, **2d**, **2e** and **2f**) were measured in chloroform with a Mass Spectrometer API 2000. Rf values were determined on TLC plates using a mixture of DCM/MeOH (96:4) as eluent.

General procedures for the synthesis of compounds 2a-s

Pathway i) Synthesis of [4-(4-fluorobenzyl)piperazin-1-yl]methanone derivatives 2a-e, 2k-m, 2q-s and 4-(4-fluorobenzyl)piperazin-1-yl]ethanone derivative 2h. To a mixture of 1-(4-fluorobenzyl)piperazine 3 (0.5 mmol) and N,N-diisopropylethylamine (0.75 mmol) in DCM (2 mL) the suitable (hetero)aroyl chloride derivative (0.6 mmol) was added. The reaction was carried out under microwave irradiation for 10 min, at 50 °C. After turning off the reaction by addition of MeOH (2 mL), water was added and the mixture was extracted with DCM (3x5 mL). The obtained organic phase was washed with brine (3x5 mL) and dried with anhydrous Na_2SO_4. The solvent was removed under reduced pressure and the final products were purified by crystallization with Et_2O or by chromatographic column (DCM/MeOH 98:02).

For compounds **2b-e**, **2h**, **2k-l** and **2r-s** registered CAS numbers have been already assigned. However, their synthetic procedures, chemical properties and structural characterization are not available in literature, except for compounds **2d** and **2k** [23]

Pathway ii) Synthesis of [4-(4-fluorobenzyl)piperazin-1-yl]methanone derivatives 2f-g, 2j, 2n-p and 4-(4-fluorobenzyl)piperazin-1-yl]ethanone derivative 2i. A mixture of the suitable carboxylate derivative (1.2 mmol), N,N,N',N'-tetramethyl-O-(1H-benzotriazol-1-yl)uronium hexafluorophosphate (HBTU) (1 mmol) in DMF (4 mL) was stirred at room temperature for 1 h. Then, a solution of the 1-(4-fluorobenzyl)pyperazine (1 mmol) in TEA (1 mmol) was added dropwise. The reaction was carried out under microwave irradiation for 10 min at 50 °C. Then, it is quenched with water (10 mL) and extracted with DCM (3x5 mL). The organic phase was dried with Na_2SO4 and the solvent was removed in vacuo. The residues were then purified by crystallization with Et_2O or by chromatographic column (DCM/MeOH 98:02), leading to the final compounds. For compound 2o registered CAS number have been already assigned. However, its synthetic procedure, chemical properties and structural characterization are not available in literature.

[4-(4-Fluorobenzyl)piperazin-1-yl](naphthalen-1-yl)methanone (2a)

Yield 88%. Oily residue. Rf = 0.49 1H-NMR (CDCl3): δ=2.26 (m, 2H, CH2), 2.58 (m, 2H, CH2), 3.19 (m, J=5.0, 2H, CH2), 3.48 (s, 2H, CH2), 3.95 (mc, 2H, CH2), 6.98 (t, J=8.7, 2H, ArH), 7.25 (t, J=8.7, 2H, ArH), 7.47 (mc, 4H, ArH), 7.87 (mc, 3H, ArH). Anal. Calcd for C22H21FN2O: C 75.84, H 6.08, N 8.04. Found: C 75.74, H 5.88, N 8.20.

[4-(4-Fluorobenzyl)piperazin-1-yl](naphthalen-2-yl)methanone (2b)

CAS number: 945155-78-2. Yield 75%. White solid. Rf = 0.48. M.p. 120-121 °C. ^{1}H NMR ($CDCl_3$): δ=2.40 (mc, 4H, CH_2), 3.48 (mc, 2H, CH_2), 3.51 (s, 2H, CH_2), 3.84 (mc, 2H, CH_2), 7.00 (t, J = 8.5, 2H, ArH), 7.28 (t, J = 8.5, 2H, ArH), 7.50 (mc, 3H, ArH), 7.87 (mc, 4H, ArH). ^{13}C NMR ($CDCl_3$): δ=52.88, 53.22, 62.07, 115.06, 115.23, 124.31, 126.68, 126.87, 126.90, 127.05, 127.78, 128.28, 128.37, 130.50, 130.56, 132.70, 133.30, 133.65, 163.07, 170.31. MS (ESI): m/z: 348.9 [M+H+]. Anal. Calcd for C22H21FN2O: C 75.84, H 6.08, N 8.04. Found: C 75.97, H 5.98, N 7.90.

[4-(4-Fluorobenzyl)piperazin-1-yl](thiophen-2-yl)methanone (2c)

CAS number: 797813-02-6. Yield 85%. Oily residue. Rf = 0.49. ^{1}H NMR ($CDCl_3$): δ=2.46 (t, J=5.0, 4H, CH_2), 3.50 (s, 2H, CH_2), 3.74 (t, J=5.0, 4H, CH_2), 7.02 (mc, 3H, ArH), 7.27 (mc, 3H, ArH), 7.43 (dd, J= 5.0 J=1.0 , 1H, ArH). Anal. Calcd for C16H17FN2OS: C 63.14, H 5.63, N 9.20. Found: C 63.25, H 5.53, N 9.18.

[4-(4-Fluorobenzyl)piperazin-1-yl](furan-2-yl)methanone (2d)

CAS number: 425397-69-9. Yield 65%. White solid. Rf = 0.41. M.p. 129-131 °C. ^{1}H NMR ($CDCl_3$): δ=2.48 (t, J=5.0, 4H, CH_2), 3.50 (s, 2H, CH_2), 3.80 (mc, 4H, CH_2), 6.45 (mc, 1H, ArH), 6.97 (mc, 1H, ArH), 7.01 (t, J=8.7, 2H, ArH), 7.28 (t, J=8.7, 2H, ArH), 7.46 (mc, 1H, ArH). ^{13}C NMR ($CDCl_3$): δ=52.96, 62.06, 111.21, 115.05, 116.23, 131.11, 133.35, 143.56, 147.98, 159.05, 163.07. MS (ESI): m/z: 289.0 [M+H+]. Anal. Calcd for C16H17FN2O2: C 66.65, H 5.94, N 9.72. Found: C 66.35, H 5.98, N 9.62.

1,3-Benzodioxol-5-yl[4-(4-fluorobenzyl)piperazin-1-yl]methanone (2e)

CAS number: 439846-81-8. Yield 74%. White solid. Rf = 0.40. M.p. 106-107°C. ^{1}H NMR ($CDCl_3$): δ=2.43 (mc, 4H, CH_2), 3.49 (s, 2H, CH_2), 3.62 (mc, 4H, CH_2), 5.99 (s, 2H, CH_2), 6.82 (d, J = 7.8, 1H, ArH), 6.91 (mc, 2H, ArH), 7.00 (t, J = 8.7, 2H, ArH), 7.28 (t, J = 8.7, 2H, ArH). ^{13}C NMR ($CDCl_3$): δ=44.46, 53.04, 62.06, 101.38, 108.06, 108.16, 115.13, 121.56, 129.42, 130.59, 133.31, 147.56, 148.76, 163.07, 169.77. MS (ESI): m/z: 342.9 [M+H+]. Anal. Calcd for C16H17FN2O2: C 66.65, H 5.94, N 9.72. Found: C 66.59, H 5.80, N 9.99.

[4-(4-Fluorobenzyl)piperazin-1-yl](1H-pyrrol-2-yl)methanone (2f)

Yield 40%. White solid. Rf = 0.29. M.p. 141-142 °C. ^{1}H NMR ($CDCl_3$): δ=2.48 (t, J=5.0, 4H, CH_2), 3.50 (s, 2H, CH_2), 3.85 (mc, 4H, CH_2), 6.23 (mc, 1H, ArH), 6.49 (mc, 1H, ArH), 6.90 (mc, 1H, ArH), 7.02 (t, J=8.5, 2H, ArH), 7.29 (t, J=8.5, 2H, ArH), 9.58 (bs, 1H, NH). ^{13}C NMR ($CDCl_3$): δ=52.97, 62.10, 109.41, 112.02, 115.11, 120.84, 124.62, 130.50, 133.38, 161.11, 163.07. MS (ESI): m/z: 288.0 [M+H+]. Anal. Calcd for C18H17FN4O5: C 66.88, H 6.31, N 14.62. Found: C 66.68, H 6.25, N 14.73.

[4-(4-Fluorobenzyl)piperazin-1-yl](1H-indol-6-yl)methanone (2g)

Yield 50%. Brown solid. Rf = 0.22. M.p. 141-142 °C. ^{1}H NMR ($CDCl_3$): δ=2.43 (mc, 4H, CH_2), 3.49 (s, 2H, CH_2), 3.60 (mc, 4H, CH_2), 6.50 (mc, 1H, ArH), 7.00 (t, J=8.7, 2H, ArH), 7.11 (d, J=8.1, 1H, ArH), 7.21 (mc, 1H, ArH), 7.27 (t, J=8.7, 2H, ArH), 7.47 (s, 1H, ArH), 7.59 (d, J=8.1, 1H, ArH),

9.31 (bs, 1H, NH). Anal. Calcd for C20H20FN3O: C 71.20, H 5.97, N 12.45. Found: C 71.10, H 5.99, N 12.10.

1-[4-(4-Fluorobenzyl)piperazin-1-yl]-2-(2-thienyl)ethanone (2h)

CAS number: 945139-36-6. Yield 35%. Oily residue. Rf = 0.43. ^{1}H NMR ($CDCl_3$): δ=2.32 (m, 2H, CH_2), 2.41 (m, 2H, CH_2), 3.45 (s, 2H, CH_2), 3.50 (m, 2H, CH_2), 3.65 (m, 2H, CH_2), 3.90 (s, 2H, CH_2), 6.88 (dd, J1=4.79, J2=1.10, 1H, H(3)-thiophene), 6.95 (dd, J1=4.79, J2=5.14, 1H, H(4)-thiophene), 7.20 (dd, J1=5.14, J2=1.10, 1H, H(5)-thiophene), 6.98-7.28 (m, 4H, ArH). Anal. Calcd. for C17H19FN2OS: C 64.13, H 6.01, N 8.80. Found: C 64.01, H 6.15, N 9.02.

1-[4-(4-Fluorobenzyl)piperazin-1-yl]-2-(2-furyl)ethanone (2i)

Yield 78%. Oily residue. Rf = 0.48. ^{1}H NMR ($CDCl_3$): δ=2.35 (m, 2H, CH_2), 2.40 (m, 2H, CH_2), 3.46 (s, 2H, CH_2), 3.52 (m, 2H, CH_2), 3.64 (m, 2H, CH_2), 3.74 (s, 2H, CH_2), 6.17 (dd, J1=3.10, J2=0.90, 1H, H(4)-furan), 6.32 (dd, J1=3.10, J2= 1.90, 1H, H(5)-furan), 6.98-7.28 (m, 4H, ArH), 7.33 (dd, J1=1.90, J2=0.90, 1H, H(2)-furan). ^{13}C-NMR ($CDCl_3$): δ=34.04, 41.89, 46.18, 52.54, 52.87, 61.93, 107.50, 110.28, 110.60, 115.04, 115.21, 130.49, 130.55, 133.26, 133.28, 141.78, 148.74, 161.11, 163.06, 167.08. Anal. Calcd. for C17H19FN2O2: C 67.53, H 6.33, N 9.27. Found: C 67.20, H 6.40, N 9.18.

Benzothiophen-2-yl-[4-(4-fluorobenzyl)piperazin-1-yl]methanone (2j)

Yield 34%. White solid. Rf = 0.66. M.p. 216-221 °C; ^{1}H NMR (DMSO-d6): δ=3.16 (m, 2H, CH_2), 3.41 (2H, CH_2) 3.51 (s, 2H, CH_2), 4.36 (s, 2H, CH_2), 4.45 (m, 2H, CH_2), 7.31-8.05 (m, 9H, Ar-H). ^{13}C NMR (DMSO-d6): δ=42.30, 46.35, 51.38, 56.04, 60.68, 115.46, 115.73, 122.55, 122.97, 125.01, 125.21, 125.91, 127.02, 130.23, 138.55, 139.40, 162.61, 163.54. Anal. Calcd. for C20H19FN2OS: C 67.77, H 5.40, N 7.90. Found: C 68.01, H 5.26, N 7.78.

Benzofuran-2-yl-[4-(4-fluorobenzyl)piperazin-1-yl]methanone (2k)

CAS number: 788097-25-6. Yield 50%. Light yellow solid. Rf = 0.65. M.p. 98 °C. ^{1}H-NMR (DMSO-d6): δ=2.43 (m, 4H, CH_2), 3.51 (s, 2H, CH_2), 3.69 (m, 2H, CH_2), 7.14-7.74 (m, 9H ArH). ^{13}C NMR (DMSO-d6): δ=44.41, 44.48, 53.16, 103.25, 103.50, 106.34, 106.77, 114.02, 115.42, 118.46, 118.75, 122.69, 122.85, 124.94, 140.01, 146.57, 151.71, 151.97, 156.56. Anal. Calcd. for C20H19FN2O2: C 70.99, H 5.66, N 8.28. Found: C 71.08, H 5.82, N 8.10.

[4-(4-Fluorobenzyl)piperazin-1-yl](3-methyl-2-thienyl)methanone (2l)

CAS number: 2337945-56-7. Yield: 82%. Oily residue. Rf = 0.52. ^{1}H-NMR ($CDCl_3$): δ=2.26 (s, 3H, CH_3), 2.44 (m, 4H, CH_2), 3.49 (s, 2H, CH_2), 3.62 (m, 4H, CH_2), 6.82 (d, J=5.0, 1H, H(4)-thiophene), 6.98-7.28 (m, 4H, ArH), 7.29 (d, J=5.0, 1H, H(5)-thiophene). ^{13}C NMR ($CDCl_3$): δ=14.79, 53.18, 62.14, 77.16, 115.19, 115.36, 125.95, 129.80, 130.40, 130.63, 130.69, 133.4, 133.47, 137.32, 161.24, 163.19, 164.66. Anal. Calcd. for C17H19FN2OS: C 64.13, H 6.01, N 8.80. Found: C 63.99, H 6.12, N 8.71.

[4-(4-Fluorobenzyl)piperazin-1-yl](4-methyl-2-thienyl)methanone (2m)

Yield 45%. White solid. Rf = 0.61. M.p. 93-95°C. 1H-NMR (DMSO-d6): δ=2.21 (s, 3H, CH_3), 2.40 (m, 4H, CH_2), 3.50 (s, 2H, CH_2), 3.62 (m, 4H, CH2), 7.15 (m, 2H, ArH), 7.20 (s, 1H, H(3)-thiophene), 7.31(s, 1H, H(5)-thiophene), 7.35 (m, 2H, ArH). ^{13}C NMR (DMSO-d6): δ=15.25, 42.30, 46.35, 51.85, 52.41, 60.76, 112.82, 114.84, 115.01, 124.58, 130.77, 131.01, 136.76, 137.03, 156.60, 160.37, 162.22 Anal. Calcd. for C17H19FN2OS: C 64.13, H 6.01, N 8.80. Found: C 64.21, H 5.93, N 8.55.

[4-(4-Fluorobenzyl)piperazin-1-yl](3-bromo-2-thienyl)methanone (2n)

Yield 99%. Oily residue. Rf = 0.71. ^{1}H-NMR ($CDCl_3$): δ=2.48 (m, 4H, CH_2), 3.48 (s, 2H, CH_2), 3.62 (m, 4H, CH_2), 6.95 (d, J=5.17, 1H, H(4)-thiophene), 6.98-7.29 (m, 4H, ArH), 7.33 (d, J=5.17, 1H, H(5)-thiophene). ^{13}C NMR ($CDCl_3$): δ=62.10, 109.74, 115.22, 115.39, 127.31, 130.30, 130.66, 132.24, 133.44, 161.27, 162.15, 163.22. Anal. Calcd. for C16H16BrFN2OS): C 50.14, H 4.21, N 7.31. Found: C 49.89, H 4.01, N 7.52.

[4-(4-Fluorobenzyl)piperazin-1-yl](5-chloro-2-thienyl)methanone (2o)

CAS number: 945107-33-5. Yield 22%. White solid. Rf = 0.66. M.p. 79-81 °C. ^{1}H NMR (DMSO-d6): δ=2.38 (m, 4H, CH_2), 3.48 (s, 2H, CH_2), 3.61 (m, 4H, CH_2), 7.13 (d, J=4.0, 1H, H(4)-thiophene), 7.14-7.36 (m, 4H, ArH), 7.29 (d, J=4.0, 1H, H(3)-thiophene). ^{13}C NMR (DMSO-d6): δ=44.39, 44.40, 53.22, 106.30, 106.73, 115.67, 118.25, 121.07, 122.64, 122.80, 134.72, 138.43, 141.68, 159.69. Anal. Calcd. for C16H16ClFN2OS: C 56.72, H 4.76, N 8.27. Found: C 56.83, H 4.52, N 8.30.

[4-(4-Fluorobenzyl)piperazin-1-yl](5-nitro-2-thienyl)methanone (2p)

Yield 55%. Brown solid. Rf = 0.72. M.p. 122-123 °C. ^{1}H-NMR (DMSO-d6): δ=2.41 (m, 4H, CH_2), 3.50 (s, 2H, CH_2), 3.61 (m, 4H, CH_2), 7.14-7.33 (m, 4H, ArH), 7.43 (d, J=4.3, 1H, H(5)-thiophene), 8.06 (d, J=4.3, 1H, H(4)-thiophene). ^{13}C-NMR (DMSO-d6): δ=42.30, 46.35, 51.85, 52.15, 60.69, 112.82, 114.84, 115.01, 128.40, 129.12, 130.73, 133.77, 143.91, 152.00, 160.06, 160.37, 162.30. Anal. Calcd. for C16H16FN3O3S: C 55.00, H 4.62, N 12.03. Found: C 54.89, H 4.58, N 11.98.

[4-(4-Fluorobenzyl)piperazin-1-yl](3-methyl-2-furyl)methanone (2q)

Yield 44%. Oily residue. Rf = 0.46. ^{1}H NMR ($CDCl_3$): δ=2.25 (s, 3H, CH_3), 2.48 (m, 4H, CH_2), 3.50 (s, 2H, CH_2), 3.71 (m, 4H, CH_2), 6.30 (bs, 1H, H(4)-furan), 6.98-7.29 (m, H, ArH), 7.3 (bs, 1H, H(5)-furan). ^{13}C NMR (DMSO-d6): δ=11.07, 50.62, 58.06, 67.03, 114.77, 115.58, 116.01, 133.68, 143.62, 159.46. Anal. Calcd. for C17H19FN2O2: C 67.53, H 6.33, N 9.27. Found: C 67.61, H 6.28, N 9.48.

[4-(4-Fluorobenzyl)piperazin-1-yl](5-methyl-2-furyl)methanone (2r)

CAS number: 945139-59-3. Yield 82%. Beige solid. Rf = 0.53. M.p. 74-78 °C. ^{1}H NMR (DMSO-d6): δ=2.29 (s, 3H, CH_3), 2.37 (m, 4H, CH_2), 3.48 (s, 2H, CH_2), 3.63 (m, 4H, CH_2), 6.21 (d, J=3.15, 1H, H(4)-furan), 6.84 (d, J=3.15, 1H, H(3)-furan), 7.14-7.35 (m, 4H, ArH). ^{13}C NMR (DMSO-d6): δ=13.35, 42.30, 46.35, 51.85, 52.53, 60.85, 107.58, 114.82, 114.99, 116.84, 130.74, 133.85, 145.40, 153.89, 158.25, 160.37, 162.30. Anal. Calcd. for C17H19FN2O2: C 67.53, H 6.33, N 9.27. Found: C 67.80, H 6.50, N 9.21.

[4-(4-Fluorobenzyl)piperazin-1-yl](5-nitro-2-furyl)methanone (2s)

CAS number: 831204-02-5. Yield 80%. Yellow solid. Rf = 0.66. M.p. 117-120 °C. ^{1}H NMR (DMSO-d6): δ=2.41 (m, 4H, CH_2), 3.50 (s, 2H, CH_2), 3.64 (m, 4H, CH_2), 7.11-7.34 (m, 4H, ArH), 7.24 (d, J=3.9, 1H, H(3)-furan), 7.73 (d, 1H, J=3.9, 1H, H(4)-furan). ^{13}C NMR (DMSO-d6): δ=42.30, 46.35, 51.85, 52.69, 60.68, 112.82, 114.85, 115.02, 116.93, 130.74, 133.78, 147.61, 151.16, 156.60, 160.37, 162.30. Anal Calcd. for C16H16FN3O4: C 57.66, H 4.84, N 12.61. Found: C 57.58, H 4.71, N 12.33.

Mushroom tyrosinase inhibition assay

Mushroom tyrosinase (EC 1.14.18.1) was purchased from Sigma Chemical Co. (St. Louis, MO, USA). Tyrosinase inhibition was assayed

according to the method of Ferro et. al. [16] with minor modifications. [24] Briefly, aliquots (0.05mL) of sample at various concentrations (2 – 80 µM) were mixed with 0.5 mL of L- tyrosine or L-DOPA solution (1.25 mM), 0.9 mL of sodium acetate buffer solution (0.05 M, pH 6.8) and preincubated at 25 °C for 10 min. Then 0.05 mL of an aqueous solution of mushroom tyrosinase (333 U/mL) was added last to the mixture. This solution was immediately monitored for the formation of dopachrome by measuring the linear increase in optical density at 475 nm for 2 minutes using an UV-vis spectrophotometer (Shimadzu UV-1601, Kyoto, Japan). DMSO was used as a negative control and Kojic acid [5-hydroxy-2-(hydroxymethyl)-4H-pyran-4-one], a fungal secondary metabolite used as skin whitening agent, was employed as a positive standard (2 – 30 µM). The extent of inhibition by the addition of samples is expressed as inhibition percentage and calculated as follows:

Inhibition %=(A-B/A)x 100

A= absorbance at 475 nm of negative control.

B= absorbance at 475 nm of test sample.

The concentrations leading to 50% activity lost (IC_{50}) were also calculated by interpolation of the dose-response curves.

Docking simulation and binding free energy calculation

Docking studies were performed by Gold suite 5.7.1.[20] using the structural coordinates of *Agaricus bisporus* tyrosinase in complex with the inhibitor tropolone (PDB code 2Y9X) [19]. The ligand and water molecules were removed and hydrogens were added by Discovery Studio 2.5.5.[25] The ligand structures were constructed using Discovery Studio 2.5.5 and energy optimized employing the Smart Minimizer protocol (1000 steps) which combines the Steepest Descent and the Conjugate Gradient methods. CHARMm was used as force field for the energy minimization. Docking simulation was performed by using the same protocol as reported in our previous paper [17]. Briefly, the binding site was defined in order to contain the residues within 15Å from the position of the ligand in the x-ray structure. A scaffold constraint was applied to restrict the solutions in which the 4-fluorophenyl fragment matches its binding pose upon the cocrystal structure of the active portion of inhibitors. [12] The side chains of residues His244, Val248, His251, Met257, Asn260, Thr261, Phe264, Arg268 and Leu275 were set as flexible and ChemPLP was chosen as fitness function. For each ligand 100 genetic algorithms runs were performed. Results differing less than 0.75 Å in terms of RMSD were clustered together. The binding conformations corresponding to the most populated cluster were chosen for analysis and representation. The obtained ligand-protein complexes were optimized by running 1000 steps energy minimization performed by means of NAMD 2.13. [26] Copper ions were replaced by zinc ions as there are no parameters available for copper ions in CHARMM22 used as force field. During the simulation, zinc ions were kept fixed while harmonic constraints were applied to the histidine residues 61, 85, 94, 259, 263 and 296 involved in the coordination of the two copper ions. The binding free energy of the protein-ligand complexes were calculated by using MM-GBSA method as implemented in AMBER18 program. [27] General Amber force field (GAFF) [28] parameters were assigned to the ligands, while partial charges were calculated by the AM1-BCC method as implemented in Antechamber. The protein was parameterized by using ff14SB force field. [29] Solvent effects were taken into account by employing the generalized Born implicit solvent model while the nonpolar part of the solvation energy is dependent on the solvent accessible surface area (SA).[30]

Cell viability assay

The human cervical carcinoma HeLa cell line was used in the cytotoxic activity assay. All cells were cultured in DMEM medium supplemented with 10% fetal bovine serum (FBS), 2 mM L-Glutamine, penicillin (100U/mL) and streptomycin (100 µg/mL) at 37 °C in a humidified atmosphere with 5% CO2. The cell survival assay was performed using colorimetric 3-(4,5-dimethylthiazol-2-yl)-2,5-diphenyltetrazolium bromide (MTT) method. Briefly, 100 µL suspended cells at an initial density of 3 × 104/mL were seeded into each well of 96-well culture plates and allowed to adhere for 24 h before addition of compounds. HeLa cell line was exposed for 48 h to compounds at concentration ranging from 4 to 100 µM for compound 2c ad from 5 to 100 µM for compound 2d. Since DMSO was used as solvent for compounds, cell viability was evaluated also in the presence of DMSO alone, as solvent control. After incubation time, culture supernatants were removed and exchanged with medium containing 0.5 mg/mL MTT. Then, after 3h incubation at 37 °C, the medium was removed, and the cells were lysed with 100 µL of DMSO. The optical density was measured at 570 nm with an auto microplate reader (Infinite 200, Tecan, Austria). The mean value and standard deviation (SD) were calculated from triplicate experiments.

Acknowledgements

This work was supported by the MIUR - "Finanziamento delle Attività Base di Ricerca" FFABR funding 2017.

Conflict of interest

The authors declare no conflict of interest.

Keywords: drug design • docking studies • MTT assay • structure-activity relationship • tyrosinase inhibitors

[1] S. Kumari, S. Tien Guan Thng, N. Kumar Verma, H. K. Gautam, *Acta Derm Venereol* **2018**, *98*, 924-931.
[2] K. Haldys, W. Goldeman, M. Jewginski, E. Wolinska, N. Anger-Gora, J. Rossowska, R. Latajka, *Bioorg Chem* **2020**, *94*, 103419.
[3] M. Brenner, V. J. Hearing, *Photochem Photobiol* **2008**, *84*, 539-549.
[4] T. Pillaiyar, V. Namasivayam, M. Manickam, S. H. Jung, *J Med Chem* **2018**, *61*, 7395-7418.
[5] I. Carballo-Carbajal, A. Laguna, J. Romero-Giménez, T. Cuadros, J. Bové, M. Martinez-Vicente, A. Parent, M. Gonzalez-Sepulveda, N. Peñuelas, A. Torra, B. Rodríguez-Galván, A. Ballabio, T. Hasegawa, A. Bortolozzi, E. Gelpi, M. Vila, *Nat Commun* **2019**, *10*, 973.
[6] K. Georgousaki, N. Tsafantakis, S. Gumeni, I. Gonzalez, T. A. Mackenzie, F. Reyes, C. Lambert, I. P. Trougakos, O. Genilloud, N. Fokialakis, *Bioorg Med Chem Lett* **2020**, *30*, 126952.
[7] H. J. Jung, S. G. Noh, Y. Park, D. Kang, P. Chun, H. Y. Chung, H. R. Moon, *Comput Struct Biotechnol J* **2019**, *17*, 1255-1264.
[8] C. Honisch, A. Osto, A. Dupas de Matos, S. Vincenzi, P. Ruzza, *Food Chem* **2020**, *305*, 125506.
[9] Y. Yuan, W. Jin, Y. Nazir, C. Fercher, M. A. T. Blaskovich, M. A. Cooper, R. T. Barnard, Z. M. Ziora, *Eur J Med Chem* **2020**, *187*, 111892.
[10] Z. Shen, Y. Wang, Z. Guo, T. Tan, Y. Zhang, *J Enzyme Inhib Med Chem* **2019**, *34*, 1633-1640.
[11] S. Vittorio, T. Seidel, M. P. Germano, R. Gitto, L. Ielo, A. Garon, A. Rapisarda, V. Pace, T. Langer, L. De Luca, *Mol Inform* **2019**.
[12] S. Ferro, B. Deri, M. P. Germano, R. Gitto, L. Ielo, M. R. Buemi, G. Certo, S. Vittorio, A. Rapisarda, Y. Pazy, A. Fishman, L. De Luca, *J Med Chem* **2018**, *61*, 3908-3917.
[13] S. Zolghadri, A. Bahrami, M. T. Hassan Khan, J. Munoz-Munoz, F. Garcia-Molina, F. Garcia-Canovas, A. A. Saboury, *J Enzyme Inhib Med Chem* **2019**, *34*, 279-309.
[14] M. J. Matos, C. Varela, S. Vilar, G. Hripcsak, F. Borges, L. Santana, E. Uriarte, A. Fais, A. Di Petrillo, F. Pintus, B. Era, *Rsc Adv* **2015**, *5*, 94227-94235.
[15] S. Ferro, L. De Luca, M. P. Germano, M. R. Buemi, L. Ielo, G. Certo, M. Kanteev, A. Fishman, A. Rapisarda, R. Gitto, *Eur J Med Chem* **2017**, *125*, 992-1001.

[16] S. Ferro, G. Certo, L. De Luca, M. P. Germano, A. Rapisarda, R. Gitto, *J Enzyme Inhib Med Chem* **2016**, *31*, 398-403.
[17] L. Ielo, B. Deri, M. P. Germano, S. Vittorio, S. Mirabile, R. Gitto, A. Rapisarda, S. Ronsisvalle, S. Floris, Y. Pazy, A. Fais, A. Fishman, L. De Luca, *Eur J Med Chem* **2019**, *178*, 380-389.
[18] G. Wolber, T. Langer, *J Chem Inf Model* **2005**, *45*, 160-169.
[19] W. T. Ismaya, H. J. Rozeboom, A. Weijn, J. J. Mes, F. Fusetti, H. J. Wichers, B. W. Dijkstra, *Biochemistry-Us* **2011**, *50*, 5477-5486.
[20] G. Jones, P. Willett, R. C. Glen, A. R. Leach, R. Taylor, *J Mol Biol* **1997**, *267*, 727-748.
[21] S. Fogal, M. Carotti, L. Giaretta, F. Lanciai, L. Nogara, L. Bubacco, E. Bergantino, *Mol Biotechnol* **2015**, *57*, 45-57.
[22] T. Mann, W. Gerwat, J. Batzer, K. Eggers, C. Scherner, H. Wenck, F. Stäb, V. J. Hearing, K. H. Röhm3, L. Kolbe, *J Invest Dermatol* **2018**, *138*, 1601-1608.
[23] S. Laufer, F. Lehmann, *Bioorg Med Chem Lett* **2009**, *19*, 1461-1464.
[24] A. Smeriglio, V. D'Angelo, M. Denaro, D. Trombetta, F. M. Raimondo, M. P. Germano, *Chem Biodivers* **2019**, *16*, e1900314.
[25] *Discovery Studio 2.5.5 Accelrys http://www.accelrys.com., in, San Diego, CA, 2009*.
[26] J. C. Phillips, R. Braun, W. Wang, J. Gumbart, E. Tajkhorshid, E. Villa, C. Chipot, R. D. Skeel, L. Kale, K. Schulten, *J Comput Chem* **2005**, *26*, 1781-1802.
[27] D.A. Case, I.Y. Ben-Shalom, S.R. Brozell, D.S. Cerutti, T.E. Cheatham, III, V.W.D. Cruzeiro, T.A. Darden, R.E. Duke, D. Ghoreishi, M.K. Gilson, H. Gohlke, A.W. Goetz, D. Greene, R Harris, N. Homeyer, Y. Huang, S. Izadi, A. Kovalenko, T. Kurtzman, T.S. Lee, S. LeGrand, P. Li, C. Lin, J. Liu, T. Luchko, R. Luo, D.J. Mermelstein, K.M. Merz, Y. Miao, G. Monard, C. Nguyen, H. Nguyen, I. Omelyan, A. Onufriev, F. Pan, R. Qi, D.R. Roe, A. Roitberg, C. Sagui, S. Schott-Verdugo, J. Shen, C.L. Simmerling, J. Smith, R. SalomonFerrer, J. Swails, R.C. Walker, J. Wang, H. Wei, R.M. Wolf, X. Wu, L. Xiao, D.M. York and P.A. Kollman ,**2018**, *AMBER 2018*, University of California, San Francisco.
[28] J. Wang, R.M. Wolf, J.W. Caldwell, P.A. Kollman, D.A. Case *J Comput Chem*, **2004**, *25*, 1157-1174.
[29] J.A. Maier, C. Martinez, K. Kasavajhala, L. Wickstrom, K.E. Hauser, C. Simmerling, *J. Chem. Theory Comput.* **2015**, *11*, 3696-3713.
[30] P.A. Kollman, I. Massova, C. Reyes, B. Kuhn, S. Huo, L. Chong, M. Lee, T. Lee, Y. Duan, W. Wang, O. Donini, P. Cieplak, J. Srinivasan, D.A. Case, T.E. Cheatham 3rd, *Acc Chem Res*, **2000**, *33*, 889-897.

10.1002/cmdc.202000125

Entry for the Table of Contents

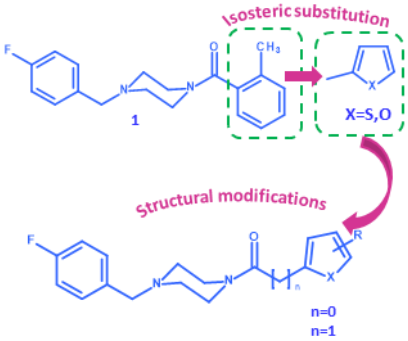

We reported the design and synthesis of a new series of tyrosinase inhibitors bearing the 4-Fluorobenzylpiperazine scaffold. The obtained compounds were tested to evaluate their ability to inhibit mushroom tyrosinase. Cytotoxicity was also evaluated for selected derivatives and docking studies were conducted to investigate their binding mode within tyrosinase catalytic pocket.